Carbon-13 Chemical Shift Tensors in Polycyclic Aromatic Compounds. 5.[1] Single-Crystal Study of Acenaphthene

Robbie J. Iuliucci, Julio C. Facelli,[†] D. W. Alderman, and David M. Grant*

Contribution from the Department of Chemistry and the Utah Supercomputing Institute, University of Utah, Salt Lake City, Utah 84112

Received September 22, 1994[⊗]

Abstract: The 36 experimentally observable ^{13}C chemical shift tensors in the acenaphthene single crystal are determined with 2D chemical shift−chemical shift correlation spectroscopy. The chemical shift tensors of the two crystallographically unique molecules in the unit cell are measured with an accuracy of 0.52 ppm. A scalar measure of the rms distance between all of the pairs of tensors in the two molecules is 1.82 ppm, indicating that single-crystal NMR measurements clearly detect the differences between the chemical shift tensors in the two molecules. To rationalize these variations, *ab initio* calculations of the ^{13}C chemical shift tensors and the derivatives of the various tensor components with respect to the molecular geometry parameters were carried out with the GIAO quantum mechanical method using the molecular structures from neutron diffraction. The calculated and experimental chemical shift tensors correlate within an rms distance of 4.99 ppm. Theoretical arguments are presented that indicate that the differences between the ^{13}C chemical shift tensors of the two unique molecules likely originate in structural variations that tend to be smaller then those detected by diffraction techniques.

1. Introduction

It is well-established that the measurement of chemical shifts in solids is a powerful tool for probing the electronic structure of molecules.[2,3] The chemical shift tensor describes the anisotropy of the chemical shift, which reflects closely the electronic structure and chemical bonding. Unlike powder studies, which provide only the three principal values of the chemical shift tensor, the directional information inherent in the full tensor, characterized by six parameters, can be obtained only from single-crystal NMR data. The enhanced resolution of 2D chemical shift−chemical shift (CS-CS) correlation spectroscopy,[4,5] with its portrayal of the shift information in a spatially correlated form, extends chemical shift tensor studies to larger molecular systems such as polycyclic aromatic hydrocarbons (PAHs). This single-crystal study demonstrates such capacity by measuring the chemical shift tensors of 36 magnetically unique carbon nuclei in the acenaphthene unit cell.

The chemical importance of PAHs, as well as the theoretical interest in their aromaticity,[6] makes fused aromatic ring systems a particularly interesting class of compounds for ^{13}C chemical shift tensor studies. The effect of ring strain on the ^{13}C chemical shift tensors of acenaphthene adds an important structural feature to the previously measured chemical shift tensors of naphthalene[7] and pyrene[8] as well as the principal values of substituted naphthalenes.[1] Furthermore, acenaphthene's unusual crystal structure incorporating two unique molecular sites in the unit cell (see Figure 1), includes a diversity of intermolecular interactions that can provide further information on the subtle dependence of ^{13}C chemical shift on slight changes in molecular geometry.[9]

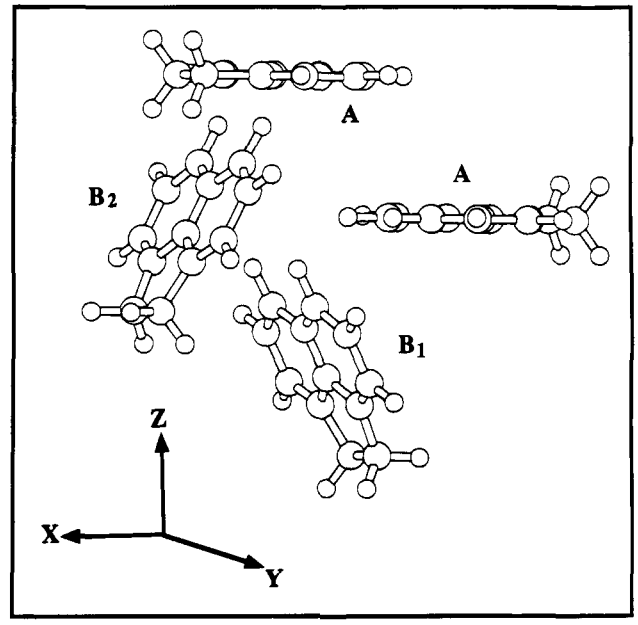

Figure 1. The unit cell, containing four molecules, can be separated into two crystallographically independent groups that are designated as A and B molecules. The two A molecules are degenerate by NMR measurements.

Crystal symmetry plays a vital role in the analysis of 2D CS-CS spectra, especially when the number of magnetically nonequivalent nuclei is larger than the number of unique

* Address correspondence to this author at the Department of Chemistry.
† Utah Supercomputing Institute.
⊗ Abstract published in *Advance ACS Abstracts*, February 1, 1995.
(1) Previous paper in this series: Orendt, A. M.; Sethi, N. K.; Facelli, J. C.; Horton, W. J.; Pugmire, R. J.; Grant, D. M. *J. Am. Chem. Soc.* **1992**, *114*, 2832.
(2) Fyfe, C. A. *Solid State NMR for Chemists*; C. F. C. Press: Guelph, 1983.
(3) Mehring, M. *High Resolution NMR in Solids*, 2nd ed.; Springer: Berlin, 1983.
(4) Carter, C. M.; Alderman, D. W.; Grant, D. M. *J. Magn. Reson.* **1987**, *73*, 114.
(5) Sherwood, M. H.; Alderman, D. W.; Grant, D. M. *J. Magn. Reson.* **1989**, *84*, 466.
(6) Garratt, P. J. *Aromaticity*; John Wiley and Sons: New York, 1986.
(7) Sherwood, M. H.; Facelli, J. C.; Alderman, D. W.; Grant, D. M. *J. Am. Chem. Soc.* **1991**, *113*, 750.
(8) Carter, C. M.; Facelli, J. C.; Alderman, D. W.; Grant, D. M. *J. Am. Chem. Soc.* **1987**, *109*, 2639.
(9) Facelli, J. C.; Grant, D. M. *Nature*, **1993**, *365*, 325.

0002-7863/95/1517-2336$09.00/0

chemical shift tensors. Due to the coincidental planarity of two of the four molecules in the unit cell, only 36 independent peaks for the 48 carbon nuclei are experimentally observable. The congruency, because of symmetry between these 36 ^{13}C resonance frequencies, further reduces the number of unique chemical shift tensors in the acenaphthene single crystal to 14. This redundancy provides a self-consistent check of the experimental results, because the carbon tensors obtained from the 36 peaks in the 2D correlation spectra must satisfy the crystalline symmetry constraints that reduce the number to the 14 unique tensors.

Finally, recent advances in computational sciences have allowed ^{13}C chemical shift tensors to be calculated with significantly improved accuracy[10] thereby assisting with the assignment and interpretation of the experimental shift tensors in acenaphthene. In this paper calculations of the derivatives of the ^{13}C chemical shift tensors with respect to molecular structure are also used to verify the significance of the difference between the tensors measured for the two structurally unique molecules in the unit cell of acenaphthene.

2. Experimental Section

1. Crystal. Acenaphthene, obtained from Aldrich, was purified by sublimation and zone refining. The Bridgman method[11] was used to grow a cylindrical single crystal 5 mm in diameter and 40 mm long. The crystal was then ground to a roughly spherical shape that filled 5 mm of a shortened 5 mm NMR tube. Epoxy glue was used to mount the crystal in a permanent position in the sample tube and to immobilize the tube in the armature of the probe.

2. Spectroscopy. Six 2D spectra were acquired at ambient temperature (~22 °C) on a Bruker CXP-200 spectrometer with operating frequencies for ^{13}C and ^{1}H of 50.304 and 200.06 MHz, respectively. A previous publication[4] describes the instrumentation including the probe, the flipping mechanism, and the pulse sequence required for the CS-CS experiment. A contact time of 3 ms was employed. The evolution time was incremented in 176 steps with 16 transients per increment, while 512 complex data points were recorded in the acquisition dimension. The 2D mixing time was 35 ms, a period adequate to rotate the sample and to allow mechanical vibrations to decay. The protons were decoupled with a field strength of 90 kHz, and a flipback pulse was used to restore the remaining proton magnetization to the longitudinal axis after the acquisition period. A recycle delay of 14 s was determined to provide the maximum signal-to-noise ratio in the allotted time of 22 h per 2D spectrum.

The set of free induction decays were transferred to a VAX 11/750 for analysis and 96 Hz Gaussian line broadening was applied. Zero filling before Fourier transformation produced a 1024 by 1024 point spectrum with a 38 462 Hz spectral width in each of the two dimensions yielding a digital resolution of 0.75 ppm. Hyper-complex data sets with quadrature detection in both the evolution and acquisition dimensions were processed to produce pure adsorption mode spectra. The highest pixel in each peak of the 2D contour plot was taken as the position of the spectral peak.

A sample of liquid tetramethylsilane (TMS) was used as an external reference. To account for differences in the magnetic susceptibilities of the flipping mechanism when the sample is reoriented between evolution and acquisition dimensions,[4] a 1D TMS reference spectrum was acquired in each orientation, to reference both dimensions. A difference, presumably due to magnetic susceptibility variations, of 1.4 ppm for the resonance frequency of TMS was observed between the two orientations. To account for magnet drift during the time required to acquire all six 2D spectra, the 1D TMS reference spectra were taken before and after acquisition of the six 2D spectra. For each sample position, the two TMS frequencies were averaged.

Using a Doty probe, the CP/MAS spectrum of acenaphthene was acquired at ambient temperature (~22 °C) on a Chemagnetics spectrometer operating at 100.02 MHz for ^{1}H and 25.152 MHz for ^{13}C. The spinning speed was 4.1 kHz, the ^{1}H decoupling field was 56 KHz, and 560 transients were accumulated.

3. Calibration of Field Directions. Previously it has been noted that minor errors in the magnetic field directions relative to the sample orientation arise from small imperfections in the flipping mechanism, and these propagate into the chemical shift tensors. For acenaphthene these systematic errors may be as large as 2 ppm and therefore it is convenient to calibrate the field directions from the redundancy associated with the crystal symmetry. The 12 corrected field directions are found by a SIMPLEX search for the minimum in the rms of the distance between the congruent chemical shift tensors.[4]

4. Quantum Mechanical Calculations. Quantum mechanical calculations of the ^{13}C chemical shift tensors were performed using the recent implementation of the GIAO method[12] in the TEXAS 93 program.[13] All the calculations were done with the D95 basis set[14] except where indicated. The molecular structures, required as input in the calculations, were from the neutron diffraction study.[15] The calculations of the chemical shifts were performed for isolated molecules without taking into account possible intermolecular interactions. The calculated values can be converted to the TMS shift scale for comparison with their experimental counterparts either by referencing them to 196.54 ppm, which corresponds to our calculated value for methane of 203.54 ppm minus the 7.0 ppm difference observed by Jameson and Jameson[16] for the shift between methane and TMS or by using the parameters of the best fit correlation between experimental and calculated tensor components as it is described below.

To explore the sensitivity of the calculated chemical shifts to the molecular geometry, their derivatives with respect to the 30 independent variables defining the molecular geometry were calculated by finite differences using increments of 0.1 Å in the bond lengths and out-of-plane deformations and 1.0° changes for in-plane angles, respectively.

3. Results and Discussion

1. Crystal Symmetry Constraints on Chemical Shift Tensors. The acenaphthene crystal belongs to the $Pcm2_1$ space group[15] with four molecules per unit cell. The crystal contains two kinds of crystallographically unique molecules, designated as A and B (see Figure 1). Thus, the symmetry operations of the space group relate only the nuclear positions either within the pair of A molecules or within the pair of B molecules. The symmetry operations in the acenaphthene crystal include a *ZX* mirror plane, a C_{2Z} screw axis and a *YZ* glide plane. The capital *X*, *Y*, and *Z* letters refer to the crystal's unit cell and lower case, *x*, *y*, and *z*, refer to the measurement or sample frame. The *ZX* mirror plane passes through the two bridgehead positions in both the A and B molecule and this reflection symmetry renders the two aromatic rings along with the two aliphatic carbons in each molecule structurally equivalent. The chemical shift tensors of any two congruent nuclei related through the *ZX* mirror plane have all their tensor elements equal except for δ_{XY} and δ_{YZ}, which must change sign to conform with the reflection symmetry. Similarly, the chemical shift tensors of the nuclei related through the *YZ* glide plane differ in signs for δ_{XY} as well as δ_{ZX}, and the C_{2Z} screw axis changes the signs of δ_{ZX} as well as δ_{YZ}. The following scheme summarizes how the off diagonal elements of the congruent tensors transform under the

(10) Grant, D. M.; Facelli, J. C.; Alderman, D. W.; Sherwood, M. H.; Nuclear Magnetic Shieldings and Molecular Structure. *Nato Advances Research Workshop*; Tossell, J., Ed.; Kluwer Academic Publishers: Dordrecht, 1993; p 367.

(11) Sherwood, J. N. In *Purification of Inorganic and Organic Materials; Techniques of Fractional Solidification*; Marcel Dekker: New York, 1969; Chapter 15.

(12) Ditchfield, R. *Mol. Phys.* **1974,** *27*, 789.

(13) Wolinski, K.; Hinton, J. F.; Pulay, P. *J. Am. Chem. Soc.* **1990**, *112*, 8251.

(14) Dunning, T. H.; Hay, P. J. *Methods of Electronic Structure Theory*; Plenum: New York, 1977.

(15) Hazell, A. C.; Hazell, R. G.; Nørskov-Lauritsen, L.; Briant, C. E.; Jones, D. W. *Acta Crystallogr.* **1986**, *C42*, 690.

(16) Jameson, A. K.; Jameson, C. J. *Chem. Phys. Lett.* **1981**, *134*, 461.

Chart 1. The Carbon Position Numbering in Acenaphthene, Which Is Identical to the Neutron Diffraction Study[14]

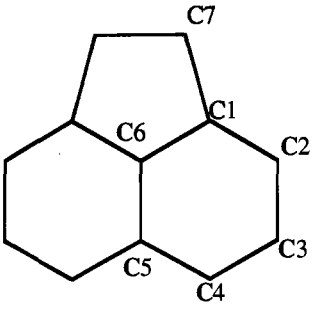

crystal symmetry in acenaphthene:

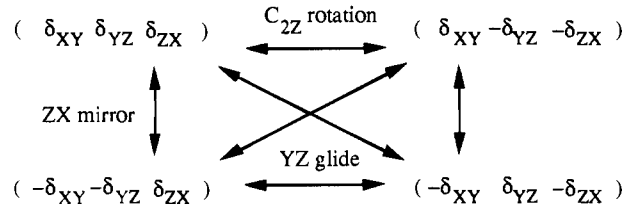

The diagonal elements are invariant under all symmetry operations of the unit cell.

Coincidentally, the C_{2Z} screw axis is perpendicular to the molecular plane of the two A molecules. To the extent that the A molecules are planar, the combination of the crystal symmetry and the planarity of the molecules creates magnetic equivalence between the two A molecules and reduces the number of observable tensors from 48 to 36. Considering the symmetry of the crystal structure, the 48 carbon nuclei in the unit cell give rise to 14 unique ^{13}C chemical shift tensors. This redundancy improves the statistical accuracy of the experimental measurements.

2. Spectral Analysis. A typical 2D CS-CS correlation spectrum of acenaphthene, one of the set of six such spectra, is shown in Figure 2. The two dimensions in the spectrum are the chemical shifts of the nuclei when the external field is in the x or zx directions of the sample frame. This spectrum, with 35 of the 36 possible peaks resolved, clearly demonstrates the increased resolution of 2D spectroscopy. The 36 ^{13}C spectral peaks pertain to 12 doubly degenerate A molecular positions and 24 magnetically different positions in each of the two congruent B molecules.

Using the six 2D spectra, shown in Figure 3, the ^{13}C chemical shifts for six different field directions were obtained. These six different field directions were the directions, x, xy, y, yz , z, and zx, in the Cartesian sample frame. This information determines the 36 experimentally observable tensors. In separate 2D spectra, sharing a common orientation of the magnetic field, the shifts of a particular nucleus will be identical. Therefore, two spectral peaks in two different spectra with the same frequency in the common dimension can be associated with one nucleus. The set of six 2D spectra includes each field direction twice and consequently correlate the directions associated with all six required frequencies measured for each nucleus. The minimal number of 2D experiments necessary to yield six unique frequencies for a specific nucleus is three, but a fourth and a fifth spectra are needed to provide the necessary correlation between the six frequencies. The sixth spectrum forms a closed path among the six spectral peaks, thus providing an additional confirmation of the association of these peaks to a particular nucleus. Figure 3 illustrates the connection of the peaks from a C-1 carbon in the A molecule through all six 2D

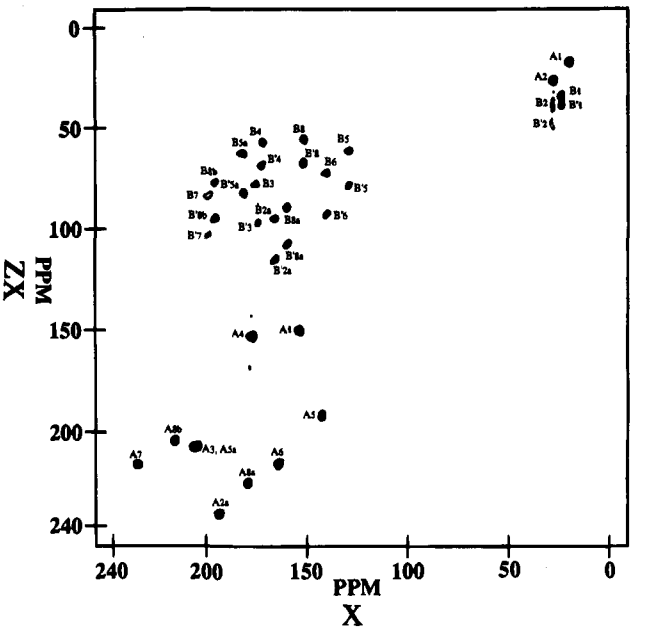

Figure 2. A typical 2D chemical shift–chemical shift correlation spectrum is shown. The spectrum shows the resonance frequencies when the magnetic field is oriented along the x or zx direction of the sample frame. The x and zx dimensions correspond to the acquisition and evolution dimension, respectively. The figure conforms to the convention of the acquisition dimension lying horizontal and the evolution dimension vertical, which places the shift of TMS in the upper right hand corner.[21]

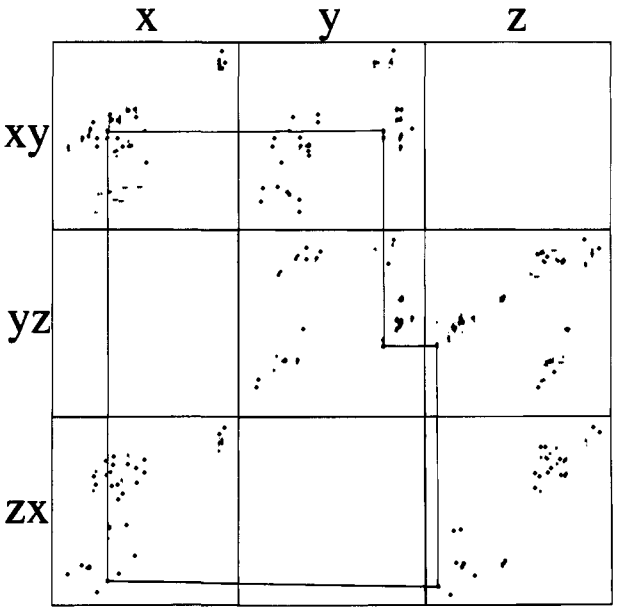

Figure 3. The complete 2D data set is shown with six spectra aligned in such a way that six spectral peaks for a single carbon nucleus can be connected to form a closed path. As explained in the text, the closure of the trace of peaks provides confirmation to the association of the six chemical shifts to the corresponding carbon nucleus. In the figure the spectral peaks corresponding to a C-1 position of the A molecule are connected. The slight tilt in the line that connects the two spectral peaks along the zx dimension corresponds to a minor misalignment of the crystal in this orientation. As explained in section 2.3, the data analysis treats this experimental imperfection. The spectra conform to the convention of the acquisition dimension lying horizontal and the evolution dimension vertical, which places the shift of TMS in the upper right hand corner in each spectrum.[21]

spectra. The minor frequency shift between the sets of spectral peaks along the zx dimension in the x–zx and z–zx spectra,

resulting in a slight tilt in the corresponding connecting line of Figure 3, reflects a minor misalignment of the crystal in the zx orientation. Such experimental imperfections appear in all peaks, though not recognizable on the spectral scale shown in Figure 3, but the redundancy in the congruent tensors is sufficient to calibrate all field directions as well as the zx orientation. Thus such probe inadequacies do not limit the accuracy of the measurement.

The 12 spectral peaks with 2-fold intensity reflect the symmetry coalescence between the resonance frequencies of the two A molecules. The coalescence is a consequence of the coincidental planarity of the two A molecules along with the C_{2Z} screw axis lying parallel to those A principal shift axes that are perpendicular to the molecular plane. Previous literature reports[6,7] on other aromatic tensors clearly establish that δ_{33} is perpendicular to the local molecular plane. Since the two A molecules are both in X-Y planes, the C_{2Z} screw axis lies perpendicular to both molecular planes and therefore is parallel within the experimental uncertainties to δ_{33} of the aromatic tensors. It is estimated that small deviations of the principal axes from the C_{2Z} axis of a half of a degree would split the aromatic spectral peaks by 1 ppm. The lack of any such splitting in the spectral peaks of the A molecule confirms, within the experimental NMR resolution, the diffraction result that all nuclei in each A molecule lie in one plane.[15] The same argument also holds for the aliphatic peaks of the A molecule except in this case it is the δ_{11} principal axis that is found to be perpendicular to the molecular plane.

The aromatic spectral peaks form patterns that reveal nominally the orientation of the molecules in the sample frame. The patterns result primarily from the similar magnitudes and orientations of δ_{33}. Seven of the ten aromatic tensors were determined to have δ_{33} within a 6.0 ppm range, five of which have the value 11.7 ± 0.3 ppm, and their directions for a given molecule are all parallel within the uncertainty of the measurement. The four molecules in the acenaphthene unit cell are contained in four planes, again the two A molecules lie in parallel X-Y planes of the crystal and the two B molecules lie in planes rotated respectively about the Y axis of the crystal by approximately $\pm 61.5°$[17] (See Figure 1). These crystal structure features explain the distinct groupings of spectral peaks found in four of the six spectra. For example, in the y magnetic field direction all ten aromatic peaks of the A molecules exhibit low shifts with a small spread in their chemical shifts, indicating that the magnetic field lies nearly along δ_{33} for this orientation. Thus, the y direction of the sample frame nearly parallels the Z axis of the unit cell frame. The yz direction in the sample frame corresponds to an orientation that is nearly perpendicular to one of the B molecules, which once again groups ten of the B spectral peaks at a low shift. Conversely the yz field direction is nearly in the molecular plane of the second B molecule as evident from their larger shifts. Thus, the spectral patterns for aromatic systems reveal the approximate orientation of the crystal in the sample frame and identify those peaks that belong to a particular molecule of the unit cell. These spectral features common to all aromatic molecules are especially useful in the single-crystal data analysis of PAHs.

3. Aromatic Tensors. a. Molecule A. The ten spectral peaks corresponding to the aromatic nuclei of the A molecules are easily recognized by their 2-fold intensity, and this tentative assignment provides a convenient starting place for the data analysis. Associating the sets of aromatic spectral peaks pertaining to the ten A tensors is straightforward, as the peaks are sufficiently dispersed that no ambiguities exist in connecting the 2D peaks around a closed path in Figure 3. The resulting ten sets of six shifts describe four pairs of congruent tensors and two unique tensors corresponding to the bridgehead positions, C-5 and C-8. The chemical shift tensors were determined using a least-squares fit of the experimental frequencies as previously described.[4] These acenaphthene tensors, reported in Table 1, are presented in the unit cell reference frame. Table 2 reports the corresponding principal values and their orientations in the molecular frame. The tensors' traces, $\delta_{ave} = (\delta_{11} + \delta_{22} + \delta_{33})/3$, are also given and compared with the isotropic values from the MAS spectrum along with the liquid values reported in the literature.[18] The agreement between solid state and liquid values substantiates the assignments of the tensors given in Tables 1 and 2. As all the isotropic shifts differ significantly from one another, the assignments may be made with confidence. Furthermore, the bridgehead tensors are easily recognized by the small anisotropy between δ_{11} and δ_{22} and by the absence of a congruent counter part. Finally, the orientation of δ_{11} in the molecular frame may be used to assign protonated aromatic carbons because it is well established[7] that δ_{11} lies almost along the C−H bonds. The 120° angle between the C-3 and C-5 C−H bond clearly differentiates between the tensors of these protonated carbons.

Table 1. ^{13}C Chemical Shift Tensors of the A and B Molecules of Acenaphthene in the Crystal Frame (All Values in ppm from TMS)

	δ_{XX}	δ_{XY}	δ_{YY}	δ_{YZ}	δ_{ZZ}	δ_{ZX}	rms[c] (ppm)
			A Molecule[a]				
C-1	238.45	−10.02	172.50	0.0	35.24	0.0	0.21
C-2	173.18	−36.61	175.07	0.0	11.39	0.0	0.30
C-3	173.65	40.34	204.79	0.0	11.87	0.0	0.44
C-4	211.15	15.35	139.16	0.0	17.21	0.0	0.25
C-5	202.07	0.0	198.75	0.0	−3.42	0.0	0.26
C-6	195.79	0.0	212.04	0.0	11.96	0.0	0.33
C-7	19.83	−5.74	22.42	0.0	30.39	0.0	0.73
			B_1 Molecule[a,b]				
C-1	81.51	−4.07	170.74	7.98	192.19	−81.06	0.36
C-2	48.80	−16.46	176.82	32.24	137.26	−65.99	0.46
C-3	46.69	19.58	202.38	−35.48	137.00	−66.64	0.60
C-4	57.70	7.90	142.91	−14.49	168.53	−78.82	0.38
C-5	41.19	0.0	198.87	0.0	156.91	−83.81	0.28
C-6	53.99	0.0	212.89	0.0	154.93	−74.41	0.41
C-7	39.02	−2.57	22.36	−5.13	26.58	−16.50	0.62

[a] The ZX reflection related pairs of C-1, C-2, C-3, C-4, and C-7 are identical in all respects except for the δ_{XY} elements, which are negated. [b] The tensors of the B_2 molecule are identical to B_1 except for the negated δ_{YZ} elements constrained by the C_{2Z} crystal symmetry. [c] The rms reported is the rms average of all identical congruent tensors.

b. Molecule B. Though the absence of coplanar B molecules reduces their relative signal to noise, it introduces beneficial redundancy into these aromatic tensors. The increased number of peaks and their reduced intensity unfortunately increases the difficulty of establishing connectivities among the six 2D experiments. The prior knowledge of the A tensors aids in establishing the correct B peak connections as the resonance frequencies of the A tensors in the orientation of the B molecules may be calculated. These predicted peaks are sufficiently close to the B peaks to enable the peak connections to be made.

Upon assigning the shifts of the A and B molecules, the symmetry constraints in the NMR data enable the establishment of the unit cell orientation relative to the sample frame. A well-conditioned least-squares fit is used to identify the transformation between the sample and unit cell frames. The symmetry constraints also resolve a number of uncertain peak assignments for the B tensors that arose from ambiguities in the simulation of the B spectral peak shifts from the rotated A tensors.

(17) Ehrlich, H. W. W., *Acta Crystallogr.* **1957**, *10*, 699.

(18) Johnson, L. F.; Jankowski, W. C. *Carbon-13 NMR Spectra*; John Wiley and Sons: New York, 1972.

4. Aliphatic Tensors. Insufficient proton decoupling power for the methylene carbons broadens the peaks and increases the uncertainty to more than 1.5 ppm in the aliphatic chemical shift tensors. When the magnetic field lies along the z direction of the sample frame, two of the six aliphatic peaks are broadened to the point that they become undetectable. The z direction of the sample frame is found to lie within 8° of one of the C-H bond vectors in the aliphatic nuclei of the B_1 and B_2 molecules, resulting in a nearly maximum dipolar interaction. While the unavailability of these data limits the accuracy of the B aliphatic tensors, there is sufficient redundancy to preserve the tensor's measurement.

Crystal symmetry reduces the minimal number of magnetic field directions required to determine completely the one unique aliphatic tensor of the B molecule to three directions. Therefore, two 2D spectra are sufficient to determine the B aliphatic tensor if proper connectivities can be established. The 16 aliphatic shifts from two spectra corresponding to the four congruent B nuclei and over determine this single unique aliphatic tensor. To capitalize on this redundancy, however, the assignments of the spectral peaks to molecular positions and the orientation of the magnetic field in the local molecular frame of the nuclei must be known. The aliphatic tensors determined by the usual method are sufficient to provide the assignment of the spectral peaks to their corresponding molecular positions and the magnetic field orientations in the molecular frames are known from the aromatic tensors analysis, which provides the directions of the magnetic field with respect to the nuclei. All observable spectral peaks are included in the analysis to fully utilize the data. A similar procedure is also used to determine the A aliphatic tensor from the two congruent A resonance frequencies with the exception that now four field directions instead of three are required to determine the one unique A aliphatic tensor. Use of redundant information reduced the uncertainty by more than a factor of 2 in both the A and B aliphatic tensors.

5. The Uncertainty in the Determination of Chemical Shift Tensors. The major source of error in the CS-CS correlation method arises from the difficulty of measuring shifts of overlapping spectral peaks. The resolution of overlapping peaks is further reduced in the evolution dimension by time restrictions on the number of evolution points which can be secured in this dimension. Often only one resonance frequency for a given dimension can be obtained from the center of a broad peak arising from two or more nuclei. Such reduced resolution explains the higher uncertainty for the C-3 tensor in the B molecules (see Table 1). In elongated overlapping peaks more than one shift frequency may be estimated. This additional degree of freedom improves the fits for the C-2 and C-3 tensors of the A molecule by a factor of about 3-fold.

A composite standard error, Δ, of the measurement may be obtained from the difference between the observed shifts and the shifts calculated from the chemical shift tensors using the symmetry relationships in the crystal. The expression is given as follows,

$$\Delta = (\sum(V_{\text{observed}} - V_{\text{tensor}})/(N - 6))^{1/2} \qquad (1)$$

where N is the number of measurements and the six represents the reduction in the number of degrees of freedom used to determine the tensor. Using eq 1, the overall composite error for acenaphthene shifts is estimated to be 0.52 ppm, and this value is sufficiently small that it may be ascribed to the experimental uncertainty in determining the resonance frequencies. The rms values for individual carbons are reported in Table 1, and the composite of these values provides an estimate of the overall error.

6. Comparison between the Tensors of the A and B Molecules. Previous work[19] introduced the concept of a scalar distance between two chemical shift tensors as a way to characterize the difference between them. This distance squared in the icosahedral representation is given by

$$D^2 = \frac{1}{6}\sum_{i=1}^{6}(X_i^{\text{A}} - X_i^{\text{B}})^2 \qquad (2)$$

where X_i^{A} and X_i^{B} are the tensor components in the icosahedral representation of the **A** and **B** tensors. For this comparison to be meaningful both tensors must be expressed in their respective molecular frames. The $\mathbf{B}_1$ tensors in the unit cell can be placed into the molecular frame of the A molecule by a rotation around the Y axis of 62.2°. This transformation corresponds to a minimization of the distance between the aromatic **A** and $\mathbf{B}_1$ tensors and was found to diagonalize the two $\mathbf{B}_1$ bridgehead tensors within experimental error. The composite calculated distances between the **A** and $\mathbf{B}_1$ tensors in their respective molecular frames is 1.82 ppm. This value is statistically significant compared with the experimental error of 0.52 ppm, as the Student t critical value for the appropriate degrees of freedom suggests that the **A** and **B** tensors are significantly different at the 99% confidence level. This analysis confirms that structural differences and/or crystalline shielding effects between these nonequivalent molecules have altered the tensors of the chemically similar positions of the A and B molecules in a measurably significant way. Conversely, the uncertainties in the neutron diffraction study failed to reveal molecular structures that are different for the crystallographically distinct A and B molecules.[15]

Shielding effects associated with intermolecular ring currents in aromatic systems fail to explain the observed differences between the tensors of the chemically similar positions of the A and B molecules. The crystal Y axis lies in the planes of both the A and B molecules, and ring currents should be nonexistent for the magnetic field oriented along the crystal Y axis. Therefore one would expect similar δ_{YY} values for the tensors of the chemically similar positions in A and B molecules, but the 3.8 ppm difference between the δ_{YY} values of the C-4 positions in these two molecules suggests that causes other than ring currents lead to this measurable shift difference (see Table 1). Furthermore, the modeling of intermolecular effects on naphthalene[9] indicates that molecular contacts need to be closer than 2.4 Å to produce a shift that exceeds 1.5 ppm. The shortest intermolecular contacts in the unit cell of acenaphthene are 2.6 Å.[17]

Table 2 further indicates that the differences between **A** and **B** tensors are in both the principal values and the tensor's orientation. The largest difference in principal values is 3.7 ppm, observed for δ_{11} at the C-1 positions, while the difference in the isotropic shifts for A and B molecules at this position is only 0.6 ppm, illustrating that structural information can be lost in standard CP/MAS NMR spectra. The largest shift distances between A and B are found at C-1, C-4, and C-7, while the smallest distances are at the C-2, C-3, C-5, and C-6 positions.

7. Theoretical Results. Theoretical methods are used to explore the possible origin of the significant differences existing between the chemical shift tensors of the A and B molecules. The inability to measure the chemical shift of the bare nucleus prevents a direct comparison of calculated shieldings to experimental shifts. Therefore, comparisons are done by correlating the relative displacements of nuclear shieldings with

(19) Alderman, D. W.; Sherwood, M. H.; Grant, D. M. *J. Magn. Reson.* **1993**, *A101*, 188.

Table 2. The Principal Values and Orientations of ^{13}C Chemical Shift Tensors of the A and B Molecules of Acenaphthene in the Molecular Frame[a,b]

	σ_{11}	σ_{22}	σ_{33}	δ_{11}	δ_{22}	δ_{33}	δ_{ave}	δ_{iso} MAS	δ_{iso} liquid[c]	δ_{11} orientation
					A Molecule					
C-1	−60.95	32.26	174.17	239.94	171.01	35.24	148.73	148.1	145.7	23.2[d]
C-2	−27.47	67.22	192.03	210.74	137.51	11.39	119.88	120.3	118.9	14.0[e]
C-3	−52.28	56.52	193.58	232.46	145.98	11.87	130.10	129.4	127.6	7.7[e]
C-4	−32.98	64.09	187.62	214.29	136.02	17.21	122.51	122.3	122.0	8.4[e]
C-5	−11.23	−7.25	218.92	202.07	198.75	−3.43	132.46	131.9	131.5	0.0[f]
C-6	−17.72	−2.60	191.39	212.04	195.79	11.96	139.93	139.9	139.1	90.0[f]
C-7	146.54	181.83	194.23	48.92	27.01	15.24	30.39	29.5	24.9	90.0[g]
					B Molecules					
C-1	−57.58	30.87	174.34	236.23	169.51	38.70	148.15	148.1	145.7	23.2[d]
C-2	−24.23	68.36	193.08	210.91	138.39	13.58	120.96	120.3	118.9	13.3[e]
C-3	−54.91	54.86	193.69	230.58	144.15	11.34	128.69	129.4	127.6	7.6[e]
C-4	−34.46	65.31	189.30	213.33	139.05	16.76	123.04	122.3	122.0	9.8[e]
C-5	−13.05	−8.18	219.98	200.89	198.87	−2.79	132.32	131.9	131.5	0.0[f]
C-6	−18.65	−0.04	192.92	212.89	194.37	14.55	140.60	139.9	139.1	90.0[f]
C-7	150.94	183.81	200.35	50.46	25.47	12.04	29.32	29.5	24.9	82.9[g]

[a] For the aromatic nuclei, δ_{33} is perpendicular to the plane of the molecule while δ_{11} and δ_{22} lie in the molecular plane. δ_{11} is perpendicular to the plane of the molecule for the aliphatic nuclei. [b] The experimental values, δ_{ii}, are in ppm referenced from TMS and the calculated values, σ_{ii}, are reported in ppm from the bare nucleus. The relationship of the best linear fit between calculated and experimental values is $\sigma = -1.10\delta + 209.84$ ppm. The intercept value would correspond in the ideal case to the absolute shielding of TMS. This equation corresponds to the correlation for the aromatic carbons of the A molecule. The fitting parameters for the B molecule are within experimental error of those for the A molecule, but inclusion of the aliphatic tensors degrades the fit significantly. [c] Liquid values from ref 18 were measured in $CDCl_3$ and reported relative to TMS. [d] Orientation in degrees relative to the C−CH_2 bond. [e] Orientation in degrees relative to the C−H bond. [f] Orientation in degrees relative to the bridgehead bond. [g] Orientation in degrees relative to the aromatic plane.

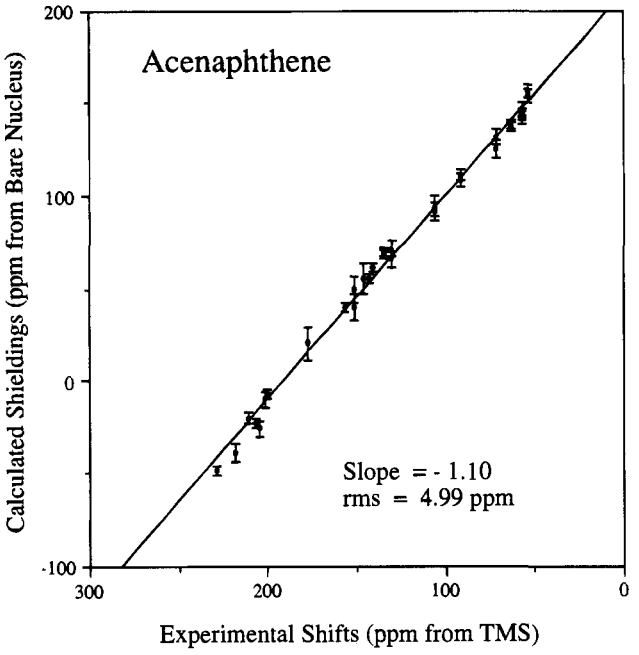

Figure 4. The correlation between the experimental tensor elements and the calculated tensor elements is shown. The experimental tensors correspond to the A molecule and the calculations use geometry inputs from neutron diffraction for the A molecules. The tensor elements are in the icosahedral representation[19] and are referenced to the bare nucleus for the calculated shieldings and to TMS for the experimental shifts. The best fit line has a slope of −1.10, an intercept of 209.84 and an rms of 4.99 ppm. The error bars estimate the propagation of the uncertainty in the geometry parameters into the calculated tensor elements.

the experimental chemical shifts. Figure 4 presents the correlation between the GIAO calculated shieldings for the aromatic carbon of the A molecule and the corresponding experimental shifts. These calculations use the geometry parameters as determined by neutron diffraction.[15] The shielding correlation plot shows a slope of −1.10 and intercepts the zero chemical shift of TMS at 209.84 ppm. The lack of a unit slope is an indication of deficiencies in the analysis. Possible limitations include the need for a better way to reference the bare nucleus, to include electron correlation in the theoretical methods, and to correct for thermal motions on the experimental shifts. Similar correlation between experimental shifts and calculated shielding tensors for the B molecule gives an rms fit of 5.06 ppm, indicating that the two fits have the same general quality, but unfortunately the calculations using the neutron diffraction data cannot identify the reasons for the measurable difference in the chemical shifts of the two molecules. This is not too surprising in that the diffraction results fail to indicate any differences between the molecular geometries of A and B that exceed the experimental diffraction error. Moreover, calculations with larger basis sets (D95* and D95**)[14] performed for the A molecule geometry do not improve the rms fit significantly. These observations suggest that the errors in the molecular geometry used in the calculations may be one of the limiting factors in the quantum mechanical calculations. Similar conclusions were reached from the single-crystal NMR studies of naphthalene[9] where the chemical shift tensors were found to deviate significantly from the D_{2h} symmetry consistent with the diffraction bond parameters.

Errors induced in the quantum calculations by uncertainties in the molecular geometries may be estimated with a set of derivatives, $\partial\delta_i/\partial p_j$, of the shift tensor components with respect to the structural parameters defining the geometry of the molecule. Thirty derivatives corresponding to changes in the bond lengths, bond angles, and out-of-plane deformations in the molecular structure were calculated. The size of the derivatives varied up to 300 ppm per Å and up to 11 ppm per deg for C−C bond lengths and C−C−C bond angles, respectively. The out-of-plane deformations of the hydrogens accounted for derivatives that ranged up to 110 ppm per Å.

The corresponding uncertainty in each of the calculated shift elements, $\Delta\delta_i$, was estimated by

$$\Delta\delta_i = (\sum_j ((\partial\delta_i/\partial p_j)^2 \Delta p_j^2))^{1/2} \quad (3)$$

where the sum spans the 30 structural parameters required to

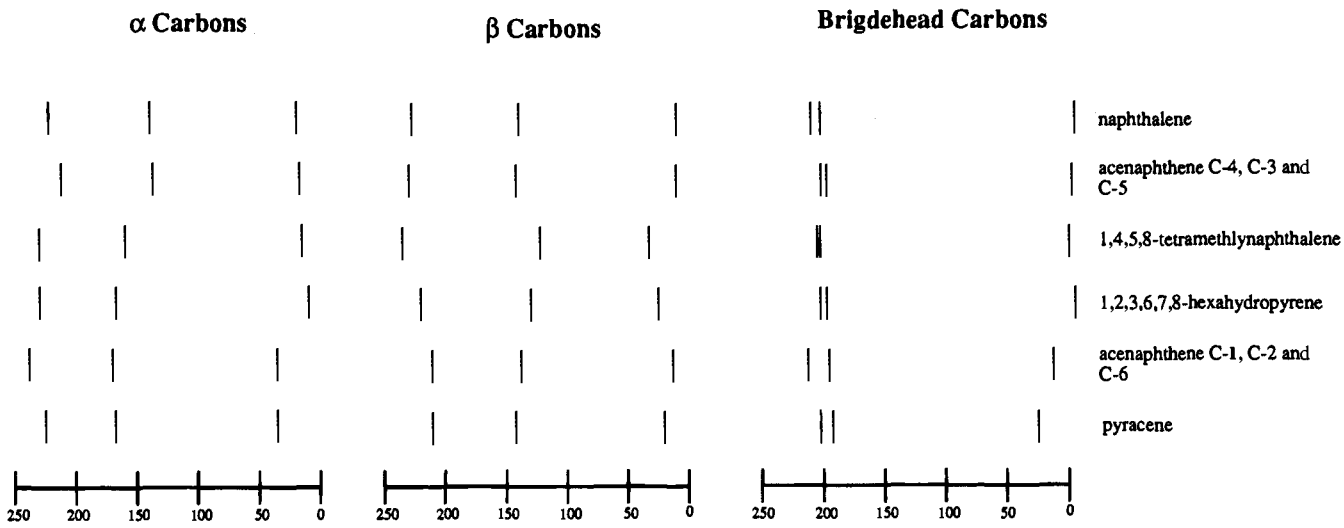

Figure 5. The principal values of the α, β, and bridgehead positions are compared graphically in acenaphthene, naphthalene,[6] 1,4,5,8-tetramethlynaphthalene,[18] 1,2,3,6,7,8-hexahydropyrene,[18] and pyracene.[18]

specify all possible acenaphthene deformations. The Δp_j are one marginal standard deviation reported in the neutron diffraction study for the uncertainties in the structural parameters.[15] The calculated $\Delta\delta_i$ ranges from 1.1 to 4.5 ppm and they are shown in Figure 4 as error bars in the calculated values of the chemical shifts. From these propagated errors in the shielding calculation, it is apparent that the scatter between the calculated and experimental chemical shifts may be attributed largely to variations introduced in the calculations by uncertainties in the molecular geometries.

8. Chemical Shift Principal Values. In Figure 5 the principal values of the chemical shift tensors in acenaphthene are compared with those of 1,4,5,8-tetramethylnaphthalene,[8] 1,2,3,6,7,8-hexahydropyrene,[8] pyracene[8] and naphthalene,[6] taken from the literature.

The effect of ring strain on the chemical shift tensors is evident for the in-plane anisotropy of the bridgehead, BH, tensors. The angles between the BH and two α positions are 126.8°,[15] 121.6°,[20] 116.5°,[8] and 111.6° [15] for acenaphthene C-5, naphthalene, pyracene, and acenaphthene C-6, respectively, and the in-plane anisotropy, δ_{11}-δ_{22} increases monotonically in this series of compounds by 3, 7, 10, and 17 ppm, respectively. The effect of ring strain at the acenaphthene C-6 bridgehead position is observed in the unusually large δ_{ave} shift, which is mostly due to the large δ_{11} and δ_{33} principal values.

The difference between the two types of α positions in acenaphthene, C-1 and C-4, is dominated by the substitution effect of the alkyl ring, resulting in the 20 ppm increased shift of δ_{22} in C-1 versus C-4. Similar to the bridgeheads, the ring strain at C-1 increases the δ_{11} and δ_{33} shifts. A combination of both the substituted and ring strain results in the unique δ_{ave} of 148.4 ppm for this C-1 carbon.

The most interesting comparison of principal values for the molecules in Figure 5 is at the β positions, where the tensors C-2 and C-3 are measurably different from each other in a manner similar to the differences in the corresponding β positions in pyracene and naphthalene. For example, the principal value comparisons of Figure 5 clearly show that the C-2 and C-3 tensors in acenaphthene reproduce the pyracene and naphthalene β principal values. The shift distance, assuming an identical principal axis frame,[19] is 4.3 ppm between C-2 and the β position of pyracene and 3.6 ppm between the C-3 and the β position of naphthalene, whereas the shift distance between C-2 and C-3 in acenaphthene is 10.8 ppm. This large shift distance is due primarily to the 20.7 ppm difference between the δ_{11} values of C-2 and C-3. Comparisons of the β positions with the remaining PAHs suggest that this δ_{11} shift is probably due to the angular strain in the adjacent five-member ring.

9. Principal Axis Orientations. For an isolated planar aromatic molecule, δ_{33} is perpendicular to the molecular plane and therefore the direction of this component should be parallel or nearly parallel for all aromatic nuclei in the molecule. The degeneracy of all resonance frequencies in the two A molecules in the crystal clearly indicates that all δ_{33} are perpendicular to the molecular plane and within experimental uncertainty, lie along the Z axis of the unit cell. The B molecules' herringbone configuration about the C_{2Z} axis of the unit cell forms two sets of δ_{33} orientations relative to each molecule. Since the two sets of six aromatic δ_{33} orientations are parallel within the experimental uncertainty, the tensor data suggest that the aromatic rings in the B molecules also exhibit no significant distortions from planarity.

Ignoring crystalline effects from neighboring molecules, the local planar symmetry of the five-member ring would also force the δ_{11} of the aliphatic carbons to be perpendicular to this ring. The coalescence of the aliphatic A spectral peaks indicates that δ_{11} is parallel to the C_{2Z} axis and therefore the five-member ring in the A molecule also lies in the same plane as the aromatic nuclei. In the case of the B molecules, however, the δ_{11} direction of the aliphatic tensors is tilted 7° toward the crystal Z axis with respect to the δ_{33} orientations of the aromatic tensors. This difference in orientation is appreciable and suggests that some form of deformation may exist in the aliphatic portion of the five-member ring of the B molecules. Preliminary analysis on modeling this δ_{11} orientation by bending the aliphatic carbons of the five-member ring from the aromatic plane indicates that the orientation of δ_{33} at the C-1 and C-6 position would also bend by up to 4°. Since all B aromatic δ_{33} are parallel within experimental uncertainty, any significant deviations of the aliphatic carbon from the plane would appear to be unlikely in agreement with the diffraction data.[15] Plausible explanations

(20) Pawely, G. S.; Yeats, E. A. *Acta Crystallogr.* **1957**, *10*, 504.
(21) Ernst, R. R.; Bodenhausen, G.; Wokaun, A. *Principles of Nuclear Magnetic Resonance in One and Two Dimensions*; Clarendon Press: Oxford, 1987.

for the observed orientation of δ_{11} in B include one or more of the following possible deformations: rotation about the Y axis of the four aliphatic protons in the ZX plane, different C−H bond lengths for geminal protons, nonperpendicular dihedral angles for the CH_2 group relative to the plane of the five-member ring, etc.

The angle between the different sets of parallel δ_{33} axes establishes the relationship between the A and B molecules and may be used to compute the molecular rotation angle about the Y axis of the unit cell frame. The average acute angle, 62.2°, between the two sets of aromatic δ_{33} axes is substantially in agreement with the 61.5° angle reported in the X-ray diffraction study.[17] This diffraction angle also presumes an effective planarity of the carbon positions.

The orientation of the two in-plane principal axes for aromatic tensors establishes that δ_{11} either lies nearly along the C−H bond or in the case of condensed carbons tends to be perpendicular to the C−C bond with the highest bond order.[7] With the exception of C-5, the acenaphthene tensors confirm this trend. In C-5, δ_{11} is oriented along the bridgehead C−C bond and fails to follow the rule. However, the $\delta_{11}-\delta_{22}$ anisotropy is sufficiently small (3 ppm for A and 2 ppm for B) that other minor electronic perturbations may account for this discrepancy. The large reported angle between the bridgehead and the two adjacent α carbons is an example of such an anomalous structural feature.

4. Conclusions.

Carbon-13 CS-CS correlation spectroscopy determines all 36 observable chemical shift tensors in acenaphthene at a reasonably high level of precision. The symmetry constraints prove to be important to the accuracy of the results by providing redundancy for congruent sets of tensors and also a self-check mechanism for the spectral peak connectivities in Figure 3. These features also establish a reliable calibration procedure for finding the field directions.

The sensitivity of the chemical shift to the electronic environment of molecules allows single-crystal studies to probe crystalline effects on molecular structure. The chemical shift rms distance of 1.82 ppm between the chemically equivalent carbon positions of the A and B molecules is more than 3 times larger than the uncertainty in the chemical shift tensor measurements and thus represents a significant difference to the tensors of the two molecules. These variations are attributed to the two different A and B crystalline environments.

Subtle changes in the local electronic structure can affect the degree of nuclear shielding as portrayed in the derivatives calculated for shifts with respect to geometry parameters. The estimation of the error in the calculated shifts, resulting from the uncertainties in the geometry parameters, equaled the scatter in the correlation plots between the calculated and experimental shift tensors. This indicates that errors in the diffraction geometries may well be one of the serious limiting factors in quantum chemical calculations of chemical shifts. Furthermore the two positions with the largest shift distance between the A and B molecules, C-1 and C-7, involve carbons in the five-member ring in which the tensors suggest that the five-member ring and/or the accompanying hydrogens deform in some way. Thus, much of the measurable shift distance between the corresponding chemical positions of the A and B molecules could result from modest structural differences, induced by crystalline packing forces, which are below the resolution of the neutron diffraction data on acenaphthene.

The experimental results presented here have not been thermally corrected: neither vibrational or rigid body motions were taken into account in the calculations. Because it is well-documented that thermal effects are important for structural determinations using diffraction methods,[22-25] the full explanation of the relationship between molecular structure and ^{13}C chemical shift tensors must await further theoretical and experimental NMR work in which thermal averaging is considered.

Some of the chemical interest in acenaphthene as a model PAHs compound is in its five-member ring. The ring strain causes increased ^{13}C shifts in δ_{11} and δ_{33} at the C-6 and C-1 positions and explains the unusual chemical shift tensors for such positions. The C-2 and C-3 chemical shift tensors closely correspond to the β tensors in naphthalene and pyracene, respectively. This similarity is interesting since the C-2 and C-3 chemical shift tensors are significantly different and reflect the domination of the local electronic structure on the tensor.

Acknowledgment. We acknowledge funding from DOE grant DE-FG02−86ER13510 and computer resources from the Utah Supercomputer Institute. The authors are grateful for a copy of the TX93 program obtained from Professors Wolinski, Hinton, and Pulay. We also thank Mark H. Sherwood for providing the single crystal and Mark Solum for acquiring the CP/MAS data given in Table 1.

JA943143S

(22) Brock, C. P.; Dunitz, J. D. *Acta Crystallogr.* **1982**, *B38*, 2218.
(23) Brock, C. P.; Dunitz, J. D. *Acta Crystallogr.* **1990**, *B46*, 795.
(24) Brock, C. P.; Dunitz, J. D.; Hirshfeld F. L. *Acta Crystallogr.* **1991**, *B47*, 789.
(25) Grant, D. M.; Liu, F.; Iuliucci, R. J.; Phung, C. G.; Facelli, J. C.; Alderman, D. W. *Acta Crystallogr. B*, in press.